*Earth Planets Space*, **51**, 979–986, 1999

# Solar radiation pressure model for the relay satellite of SELENE

Toshihiro Kubo-oka* and Arata Sengoku

*Hydrographic Department, Maritime Safety Agency, Tsukiji 5-3-1, Chuo-ku, Tokyo 104-0045, Japan*

(Received April 12, 1999; Revised September 7, 1999; Accepted September 7, 1999)

A new radiation pressure model of the relay satellite of SELENE has been developed. The shape of the satellite was assumed to be a combination of a regular octagonal pillar and a column. Radiation forces acting on each part of the spacecraft were calculated independently and summed vectorially to obtain the mean acceleration of the satellite center of mass. We incorporated this new radiation pressure model into the orbit analysis software GEODYN-II and simulated the tracking data reduction process of the relay satellite. We compared two models: one is the new radiation pressure model developed in this work and the other a so-called "cannonball model" where the shape of the satellite is assumed to be a sphere. By the analysis of simulated two-way Doppler tracking data, we found that the new radiation pressure model reduces the observation residuals compared to the cannonball model. Moreover, we can decrease errors in the estimated lunar gravity field coefficients significantly by use of the new radiation pressure model.

## 1. Introduction

SELENE (SELenological and ENgineering Explorer) is a Japanese lunar mission which is planned for launch in 2003. One of the important scientific objectives of this mission is to determine the lunar gravity field more precisely than before, especially the gravity field of the far-side of the Moon, from the orbits of two spacecraft: a lunar orbiter and a relay satellite (Matsumoto *et al.*, 1999). The lunar orbiter, the main spacecraft of the mission, is composed of a boxlike main body and a large solar panel. It carries many scientific instruments such as a laser altimeter, a magnetometer, and laser sounder. Its orbit is low ($h = 100$ km), near circular ($e \sim 0$), and almost polar ($i = 95$ deg). The relay satellite is spin-stabilized. Its shape is, roughly speaking, a combination of a regular octagonal pillar and a column (Fig. 1). Its main purpose is to relay the Doppler signal between the ground station and the lunar orbiter. It moves on an almost polar ($i = 95$ deg) and elliptical ($e \sim 0.38$) orbit with the pericenter at about 100 km altitude. The mass of the relay satellite is planned to be 39 kg.

One of the distinguishing features of SELENE is the capability of performing for-way range-rate measurements by Four-way Doppler (ground station to Relay Satellite to Orbiter to Relay Satellite to ground station). Using this method, we can directly observe the disturbance on the trajectory of the lunar orbiter when it flies over the far side of the Moon. In other words, SELENE will be the first lunar mission which will directly determine the lunar gravity field of the far side (Matsumoto *et al.*, 1999). Moreover, since the relay satellite undergoes no orbit maneuver throughout the period of the mission, the long term variations of its orbit can be observed. Then, it may be possible to determine low order gravity coefficients more precisely from the tracking data of the relay satellite.

However, in order to estimate the lunar gravity field precisely from four-way Doppler measurements and long-term variation of the relay satellite's orbit, it is indispensable to improve the orbit accuracy of the relay satellite. Because of large area to mass ratio of the relay satellite ($A/m \sim 0.017$ $m^2$/kg), the surface forces acting on the satellite are the major error source for orbit determination. Solar radiation pressure, lunar albedo radiation pressure, and thermal emission are the sources of non-gravitational perturbations acting on the satellite. Among them, solar radiation pressure is the largest non-gravitational force (Sengoku, 1998). Therefore, the study of solar radiation pressure on the relay satellite is required at the first step. A simple solar radiation model of the relay satellite was first developed by Kubo-oka (1999). In this model, the satellite was assumed simply to be a regular octagonal cylinder. In the present paper, we describe an improved radiation pressure model of the relay satellite, where the shape of the relay satellite is assumed to be more realistic: it is considered to be a combination of a regular octagonal cylinder which corresponds to the main body of the spacecraft and a column which corresponds to the docking assembly with the lunar orbiter. Differences in the optical properties between the various parts of the spacecraft are also taken into account.

Furthermore, we have implemented our new radiation pressure model of the relay satellite into GEODYN-II, an orbit analysis software developed at NASA Goddard Space Flight Center (Pavlis *et al.*, 1998). This software will be used to analyze real tracking data of SELENE spacecraft to determine the lunar gravity field. Using this modified version of GEODYN-II, tracking data reduction process of the relay satellite was simulated. Moreover, lunar gravity field estima-

*Present address: Kitamine-machi 37-7, Ohta-ku, Tokyo 145-0073, Japan.

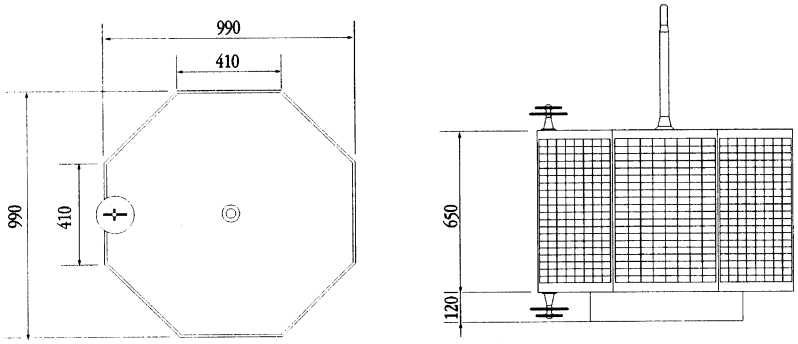


Fig. 1. Shape of the relay satellite of SELENE.

tion from the tracking data of the relay satellite was simulated by use of GEODYN-II and SOLVE (Ullman, 1992). It is the purpose of this work to investigate the effect of different radiation pressure models on the orbit of relay satellite and on the estimation of lunar gravity field coefficients.

## 2. New Radiation Pressure Model for the Relay Satellite

In this section, we will describe a new solar radiation pressure model of the relay satellite. The satellite-fixed coordinate system adopted in this work is shown in Fig. 2. We choose the $z$-axis to be parallel to the spin axis, the $x$-axis to be normal to both the spin axis and the direction to the Sun, and the $y$-axis to form a right-handed system. The angle between spin axis and the direction to the Sun is denoted by $\theta$.

We have made the following assumptions for simplicity:

1) The shape of the relay satellite is a combination of a regular octagonal pillar and a cylinder. The contribution of the antennae is neglected.

2) The rotation period is much shorter than the orbital period and the solar radiation force acting on the spacecraft is constant during the period of one rotation. In reality, the rotation period of the relay satellite is planned to be six seconds, which is much shorter than the orbital period of about 4 hours.

3) The orientation of the spin axis does not change. It is assumed to be normal to the lunar orbital plane at the time of orbit insertion. Because of the directivity of the antennae attached on the top and bottom plates, it is most favorable that the direction of the spin axis is perpendicular to the Earth-Moon line.

4) The optical properties of each surface element can be expressed by a linear combination of a black body, a perfect mirror and a Lambert diffuser (see e.g. Milani *et al.*, 1987).

5) The surface materials are chosen as follows
   - Side panels : solar cells.
   - Top and Bottom panels : gold foil.
   - Docking Assembly : gold foil.

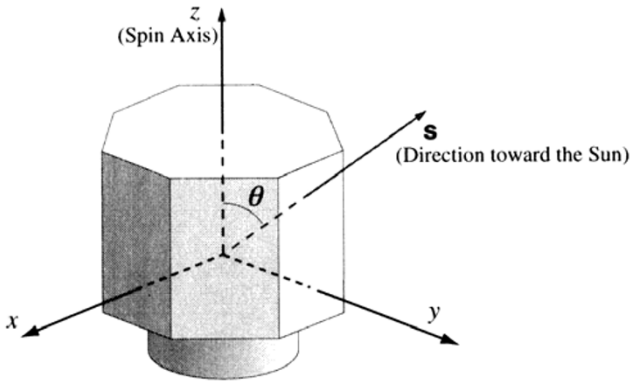


Fig. 2. Satellite-body fixed coordinate system.

6) The effects of shadowing and reflection by the different parts of the spacecraft are neglected.

First, suppose a regular pillar which has $n$ side plates. Let $A$, $\rho$, and $\delta$ be the area of single side plate, the specular reflectivity, and the diffuse reflectivity of the plate, respectively. A force acting on a flat plate can be expressed as (Milani *et al.*, 1987)

$$d\mathbf{F} = -\frac{A\Phi}{c}\left[(1-\rho)\,\mathbf{s} + 2\left(\frac{\delta}{3} + \rho\cos\beta\right)\mathbf{n}\right]|\cos\beta|\,, \tag{1}$$

where $c$, $\Phi$, $\mathbf{s}$, $\mathbf{n}$, and $\beta$ are the speed of light, the solar constant, the unit vector in the direction to the Sun, the unit vector in the direction normal to the plate, and the angle between $\mathbf{s}$ and $\mathbf{n}$, respectively. Summing up the forces acting on each plate in sunlight and averaging over the rotational period, we obtain the mean acceleration over one spacecraft rotation due to the solar radiation pressure on the $n$ side plates of the pillar as,

$$(\mathbf{a}_{\text{side}})_y = -n\frac{A\Phi}{3mc}\sin\theta\left\{\frac{3+\rho}{\pi}\sin\theta + \frac{\delta}{2}\right\}, \tag{2}$$

$$(\mathbf{a}_{\text{side}})_z = -n\frac{A\Phi}{\pi mc}(1-\rho)\sin\theta\cos\theta, \tag{3}$$

where $m$ is the mass of the relay satellite. By averaging, $x$-component which is normal to both spin axis and direction to the Sun vanishes and only $y$- and $z$-components remain.

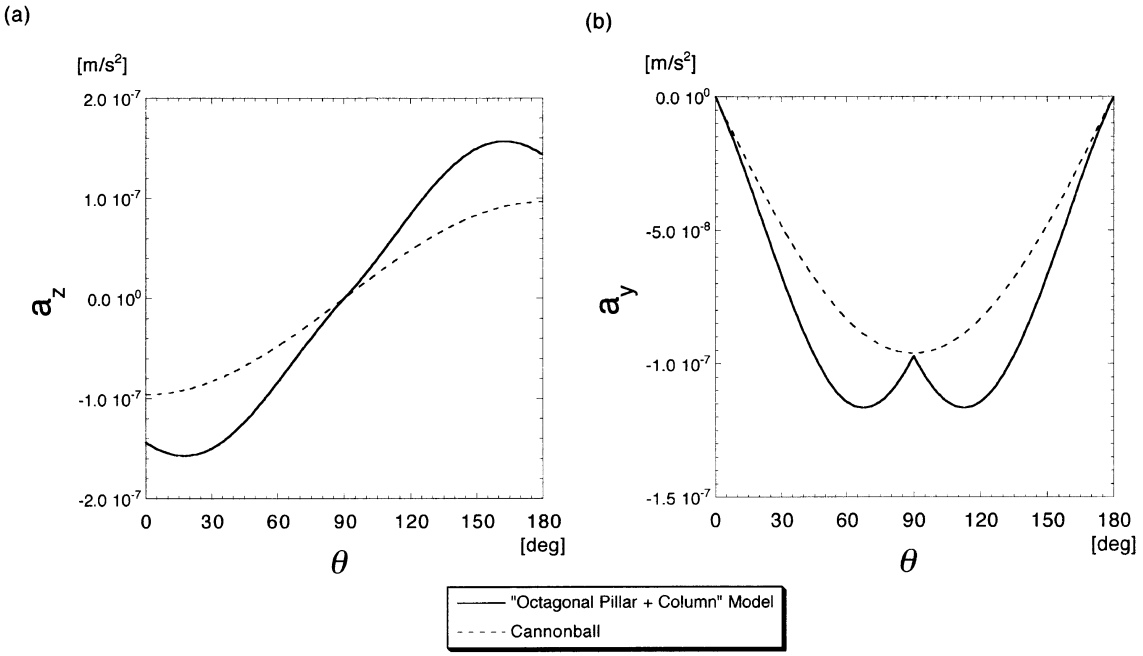


Fig. 3. Acceleration due to the solar radiation pressure: (a) component parallel to spin axis, (b) component normal to spin axis. Solid and dotted lines represent "new (octagonal pillar + column)" model and "cannonball" model, respectively.

The regular octagonal part of the relay satellite corresponds to $n = 8$ and the acceleration on them can be written as

$$(\mathbf{a}_{\rm oct})_y = -\frac{8A_{oct}\Phi}{3mc}\sin\theta\left\{\frac{3+\rho_s}{\pi}\sin\theta+\frac{\delta_s}{2}\right\}, \quad (4)$$

$$(\mathbf{a}_{\rm oct})_z = -\frac{8A_{oct}\Phi}{\pi mc}(1-\rho_s)\sin\theta\cos\theta, \quad (5)$$

where $A_{\rm oct}$, $\rho_s$, $\delta_s$ represent the area of one of the eight side plates of the octagonal pillar, the specular reflectivity, and the diffuse reflectivity of the solar cell, respectively. The docking assembly, a column, can be regarded as a limit case where $n$ tends to infinity. In general, the area of a side plate of a regular pillar which has $n$ side plates can be expressed as

$$A = 2r_{\rm c}h_{\rm c}\sin\left(\frac{\pi}{n}\right), \quad (6)$$

where $r_{\rm c}$, $h_{\rm c}$ are the radius and height of the column. Therefore, for $n \to \infty$, $nA$ converges to

$$\lim_{n\to\infty} nA = 2\pi r_{\rm c}h_{\rm c} \quad (7)$$

and the acceleration of the column may be written as

$$(\mathbf{a}_{\rm col})_y = -\frac{2\pi rh\Phi}{3mc}\sin\theta\left\{\frac{3+\rho_{\rm g}}{\pi}\sin\theta+\frac{\delta_{\rm g}}{2}\right\}, \quad (8)$$

$$(\mathbf{a}_{\rm col})_z = -\frac{2rh\Phi}{mc}\left(1-\rho_{\rm g}\right)\sin\theta\cos\theta, \quad (9)$$

where $\rho_{\rm g}$, $\delta_{\rm g}$ represent the specular and diffuse reflectivity of the gold foil. The acceleration of the top plate can be obtained from using Eq. (1) directly.

$$(\mathbf{a}_{\rm tb})_y = \begin{cases} -\frac{A_{\rm tb}\Phi}{mc}\left(1-\rho_{\rm g}\right)\sin\theta\cos\theta \\ \qquad\qquad (\text{if } \theta \le \pi/2) \\ \frac{A_{\rm tb}\Phi}{mc}\left(1-\rho_{\rm g}\right)\sin\theta\cos\theta \\ \qquad\qquad (\text{if } \theta > \pi/2) \end{cases}, \quad (10)$$

Table 1. Specular and diffuse reflectivities of the surface materials adopted in this paper (after Antreasian and Rosborough, 1992).

| Material | $\rho$ | $\delta$ |
|---|---|---|
| Solar panel | 0.042 | 0.168 |
| Gold foil | 0.184 | 0.736 |

$$(\mathbf{a}_{\rm tb})_z = \begin{cases} -\frac{A_{\rm tb}\Phi}{mc}\cos\theta\left\{\left(1+\rho_{\rm g}\right)\cos\theta+\frac{2}{3}\delta_{\rm g}\right\} \\ \qquad\qquad (\text{if } \theta \le \pi/2) \\ \frac{A_{\rm tb}\Phi}{mc}\cos\theta\left\{\left(1+\rho_{\rm g}\right)\cos\theta+\frac{2}{3}\delta_{\rm g}\right\} \\ \qquad\qquad (\text{if } \theta > \pi/2) \end{cases}, \quad (11)$$

where $A_{\rm tb}$ is the area of the top plate of the satellite. Because the effects of self-shadowing are neglected, the area of the bottom panel is considered to be equal to that of the top panel and Eqs. (10) and (11) applies to the bottom plates as well. Finally, the mean acceleration of the relay satellite due to the solar radiation pressure can be expressed as the sum of three components:

$$\mathbf{a}_{\rm total} = \mathbf{a}_{\rm oct} + \mathbf{a}_{\rm col} + \mathbf{a}_{\rm tb}. \quad (12)$$

The real optical properties of the surface materials of the relay satellite have not been measured yet. In lack of the true optical properties, the reflectivity values are adopted from a similar radiation pressure model of TOPEX/Poseidon (Antreasian and Rosborough, 1992). These values are summarized in Table 1. The ratio of specular reflectivity to diffuse reflectivity is assumed to be 1/4. Hereafter, the octagonal pillar plus column model is referred to as "new model" for simplicity.

In Fig. 3, we show the dependence of the accelerations due to the solar radiation on $\theta$. For comparison, the accel-

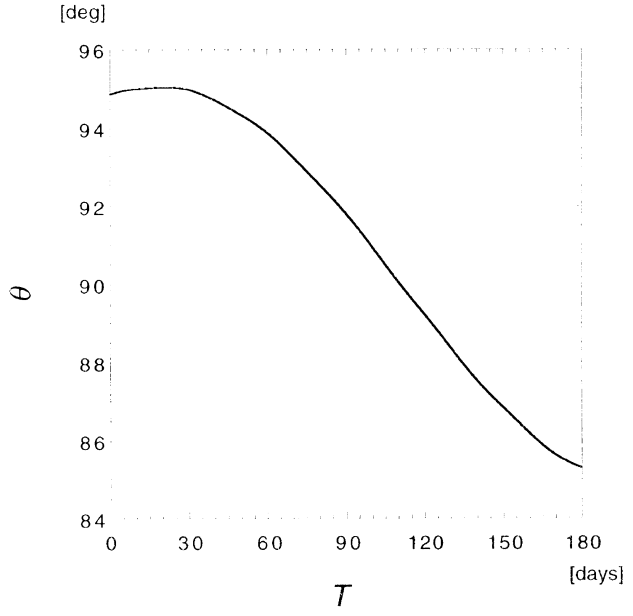


Fig. 4. Expected variation of the angle between the spin axis of the relay satellite and the direction to the sun, $\theta$, after the orbit insertion.

erations computed from so-called a "cannonball model" are also shown in the same figure in dashed lines. In the cannonball model, the satellite is assumed to be a uniform sphere and the acceleration due to the solar radiation pressure is given by

$$\mathbf{a}_{\text{total}} = -C_{\text{R}} \frac{A}{m} \frac{\Phi}{c} \mathbf{s}, \tag{13}$$

where $C_{\text{R}}$ is a radiation pressure coefficient. If the sphere reflects light specularly or diffusely, the radiation pressure coefficient can be expressed as

$$C_{\text{R}} = 1 + \frac{4}{9}\delta. \tag{14}$$

The cannonball model is commonly used as the default solar radiation pressure model in orbit analysis programs like GEODYN-II (Pavils *et al.*, 1998). In the case of the cannonball model, the $y$- and $z$-component of acceleration are sinusoidal functions of $\theta$, and, as we can see in Fig. 3, the difference in $y$-component accelerations between the new model and the cannonball case becomes largest in the vicinity of 70 deg and 110 deg. These maxima mainly due to the forces acting on the top (or bottom) plate.

In Fig. 4, we show the expected variation of $\theta$ over six months after the spacecraft is inserted into orbit. Since the orientation of the spin axis is assumed to be normal to the lunar orbital plane and since the lunar orbital plane inclines about five deg from the orbital plane of the Earth, $\theta$ varies sinusoidally between 85 and 95 deg. Even in this small range of possible values of $\theta$, the differences in acceleration calculated by the new model and the cannonball model remain. More specifically, the difference in the $z$-component rises to about 30% of its magnitude.

The component of the acceleration parallel to the direction to the Sun and its normal component as functions of $\theta$ are shown in Fig. 5. It should be noted that, in the case of the new model, the normal component yields a maximum amplitude of about 12% of the parallel component. Even in the range of 85–95 degrees range of $\theta$, the normal component becomes about 3% of the parallel component. On the contrary, in the case of the cannonball model, as can easily be derived from Eq. (13), no normal component appears and the line-of-sight component of the acceleration does not depend on $\theta$.

## 3. Simulation of the Tracking Data Reduction of the Relay Satellite

We incorporated our new radiation pressure model of the relay satellite into GEODYN-II and simulated the tracking data reduction process of the relay satellite. First, by use of this modified GEODYN-II, we simulated tracking (two-way range-rate) data for six months long. One single tracking station (NASDA Tracking and Control Center, Tsukuba, Japan) was taken into account. In Table 2, the initial orbital elements of the relay satellite used to generate tracking data are shown. The epoch corresponds to the time of deployment of the relay satellite in lunar orbit. The simulated tracking data begins at August 2, 2003 and ends at February 1, 2004. The sampling rate is 30 sec and the total number of observations is 236147. In the first half of the period (from August to October), the relay satellite is always in sunlight. During the second half of the period (November to February), the satellite occasionally enters the shadow of the Moon. Next, to make the simulation more realistic, random noise (RMS 1.0 mm/sec) was added to the simulated tracking data. This level of noise is comparable to the one expected for the real tracking data of the relay satellite.

In Table 3, we summarized the force models adopted in this work. The reference lunar gravity field model used for the analysis is LUN60d with degrees and orders up to $60 \times 60$ (Konopliv *et al.*, 1993). The product of the universal gravitational constant and lunar mass, $GM$, was taken to be $4.902797814 \times 10^{12}$ m$^3$/s$^2$. The gravitational attraction of the Earth and other planets were included. DE-403 (Standish *et al.*, 1995) was used as the ephemeris of the celestial bodies. The solar flux $\Phi$ and velocity of light $c$, which are closely related to the solar radiation pressure, were taken to be 1372.5398 W/m$^2$ and 299792458 m/s, respectively. Relativistic effects such as the general relativistic point mass acceleration were also included following McCarthy (1992). The effects of atmospheric drag and lunar albedo were neglected in this work.

We input this simulated observation data and analyzed it to determine the relay satellite orbit. Length of the arc was taken to be 1 month. Only six parameters, initial position and velocity of the spacecraft, were estimated. Since the force models and the observation models used to produce and to reanalyze the tracking data are the same, RMS of the observation residuals must be equal or very close to RMS of the noise added to the tracking data. The results of the numerical calculation were summarized in Table 4. In all cases, RMS of the observation residuals becomes less than 1.0 mm/sec. The same tracking data was also analyzed by use of the cannonball model. As we mentioned before, the "cannonball model" is incorporated as a default solar radiation pressure model in the normal version of GEODYN-II. In this case, the radiation pressure coefficient $C_{\text{R}}$ (Eq. (14)) along with

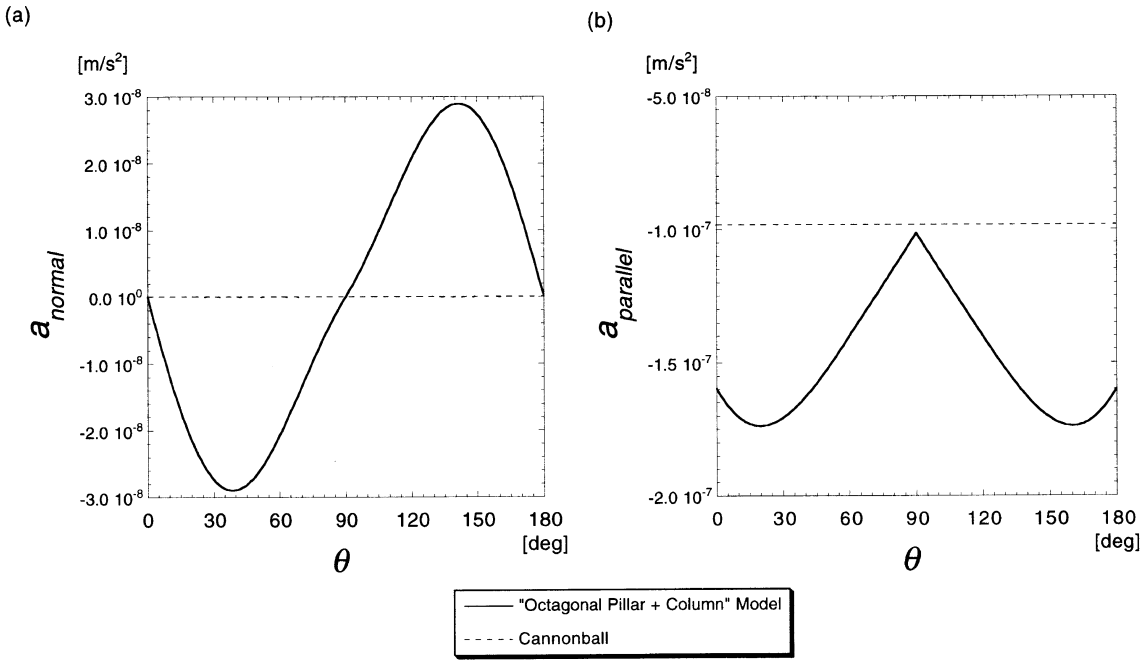


Fig. 5. Acceleration due to the solar radiation pressure: (a) component parallel to the direction to the Sun, (b) component normal to the direction to the Sun. Solid and dotted lines represent "new" model and "cannonball" model, respectively.

initial orbital state vector were estimated. $C_R$'s can be estimated at any frequency. If the observation residuals become small enough, we do not have to use any complicated solar radiation pressure model. However, it should be noted that the effect due to the gravity field may be absorbed into estimated reflection coefficient. Post-fit RMS of the observation residuals for various frequency of the estimation for $C_R$ are also shown in Table 4. RMS of the observation residuals tends to decrease as $C_R$'s are estimated more frequently. But their differences are small except for the case where $C_R$ is estimated once per month. Even if radiation pressure coefficients are estimated once per day, we cannot reduce RMS of observation residuals sufficiently, except for November, 2003. The difference between the new model and the cannonball model comes from the existence of the anisotropic component of acceleration which is perpendicular to the sun-satellite direction. As we stated in Section 2, there is a normal component in the case of the new model. On the other hand, in the cannonball model, there is no normal component of acceleration (Eq. (13)). Therefore, even if $C_R$'s are estimated very frequently, the effect due to the normal component cannot be corrected. The magnitude of the normal component is a function of $\theta$ and becomes larger as $\theta$ differs from 90 deg. In the period we considered here, it becomes largest in August, 2003 and January, 2004 (see Fig. 3). In these seasons, the sunlight incidents on the top panel as well as side panels and normal component of acceleration appears. On the contrary, in November, 2003, the sunlight incidents on the side panel almost perpendicularly ($\theta \simeq 90$ deg) and normal component of the acceleration vanishes (see Fig. 5). Therefore, post-fit RMS for cannonball model becomes very close to RMS of the noise in November. In January, 2004, the post-fit RMS for cannonball model becomes about three times as large as RMS of noise. This result comes from the fact that the normal component becomes largest and the satellite occasionally enters the shadow of the Moon in this month. As Sengoku *et al.* (1995) showed, effect of the normal component on the orbit appears more definitely during the shadowing periods. For example, averaged along-track acceleration due to normal component over one revolution doesn't vanish during the shadowing periods, and hence, the perturbation in semimajor axis appears from zero-th order in eccentricity.

Table 2. Initial orbital elements of the relay satellite at epoch August 2, 2003.

| | | |
|---|---|---|
| Semi-major axis | $a$ | 3000 km |
| Eccentricity | $e$ | 0.38 |
| Inclination | $i$ | 95° |
| Longitude of ascending node | $\Omega$ | 270° |
| Argument of pericenter | $\omega$ | 133° |
| Mean anomaly | $M$ | 0° |

## 4. Simulation of the Lunar Gravity Field Recovery

Next, we investigated how the difference in radiation pressure models affects the precision of the lunar gravity field determination. Lunar gravity field coefficients can be estimated by analyzing the tracking data of the spacecraft by use of GEODYN-II and SOLVE. GEODYN-II is used to output a normal equation matrix for each arc. The length of the arc is taken to be 1 month as before. SOLVE combines the resultant matrices of normal equations and solves them to produce lunar gravity field coefficients. Here, we combined normal equations from every arc with equal weights. The

Table 3. Adopted force models for orbit simulation analysis of the relay satellite.

| Item | Model and value | Reference |
|---|---|---|
| Lunar gravity field | LUN60d | Konopliv *et al.* (1993) |
| Planetary ephemeris | DE403 | Standish *et al.* (1995) |
| $GM$ | $4.902797814 \times 10^{12}$ m$^3$/s$^2$ | |
| Solar flux, $\Phi$ | 1372.5398 W/m$^2$ | |
| Velocity of light, $c$ | 299792458 m/s | |
| Radiation pressure model | "octagonal pillar + column" model | This paper |
| Relativistic corrections | IERS Standards | McCarthy (1992) |
| Lunar albedo | neglected | |
| Atmospheric drag | neglected | |

Table 4. Post-fit RMS of the observation residuals. From November, 2003 to January, 2004, the relay satellite occasionally enters the shadow of the Moon.

| | RMS mm/sec | | | | | |
|---|---|---|---|---|---|---|
| Estimation of $C_R$ | Aug., 2003 | Sep. | Oct. | Nov. | Dec. | Jan., 2004 |
| Cannonball model | | | | | | |
| once per 1 month | 4.171 | 2.701 | 2.680 | 14.544 | 65.102 | 119.487 |
| once per 14 days | 1.513 | 1.451 | 1.276 | 1.072 | 1.732 | 3.214 |
| once per 7 days | 1.513 | 1.457 | 1.262 | 1.029 | 1.602 | 3.139 |
| once per 2 days | 1.487 | 1.370 | 1.223 | 0.997 | 1.512 | 3.042 |
| once per 1 day | 1.473 | 1.350 | 1.218 | 0.996 | 1.436 | 2.897 |
| New model (without $C_R$ estimation) | 0.986 | 0.981 | 0.982 | 0.986 | 0.981 | 0.992 |

same simulated tracking data described in Section 3 were used as input data.

The lunar gravity field with degrees and orders up to 30 was estimated. Because of the lack of direct tracking data over the far side of the Moon, an a priori power law constraint of the form,

$$\hat{\sigma}_l = 15 \times 10^{-5}/l^2, \tag{15}$$

where $l$ is the degree of spherical harmonics, was applied to avoid that the high degree terms becomes unrealistically large (Kaula, 1966). This form of constraint is as the same as the one that Konopliv *et al.* (1993) and Lemoine *et al.* (1997) used to obtain lunar gravity field models. Analyzing the same tracking data described above, we recovered two types of lunar gravity field models: (1) coefficients estimated with new radiation pressure model and (2) coefficients by use of the cannonball model. To visualize the error in the estimated gravity field coefficients from the reference gravity field LUN60d, we calculated the following quantity $\delta_l$ defined by

$$\delta_l = \frac{\frac{1}{2l+1}\sum_m \left(\Delta C_{lm}^2 + \Delta S_{lm}^2\right)}{\hat{\sigma}_l^2}, \tag{16}$$

where $C_{lm}$ and $S_{lm}$ represent the lunar gravity field coefficients. $\Delta C_{lm}$ and $\Delta S_{lm}$ are the difference between estimated coefficients and LUN60d. This quantity can be considered to be a measure of how much the estimated coefficients of each degree differ from the reference gravity field. In Fig. 6, we show $\delta_l$ as a function of degree $l$. The results obtained with the new radiation pressure model and the cannonball model with different frequencies of the $C_R$ estimation are shown. For low degree coefficients ($l < 10$), $\delta_l$ increases steeply as the degree $l$ becomes higher. However, when degree $l$ exceeds 10, $\delta_l$ does not increase and remains in almost same order of magnitude. This is caused by a priori power law applied to solve the normal equation. For all degrees, the value of $\delta_l$ obtained by the use of the new model is much smaller than the one obtained by the use of cannonball

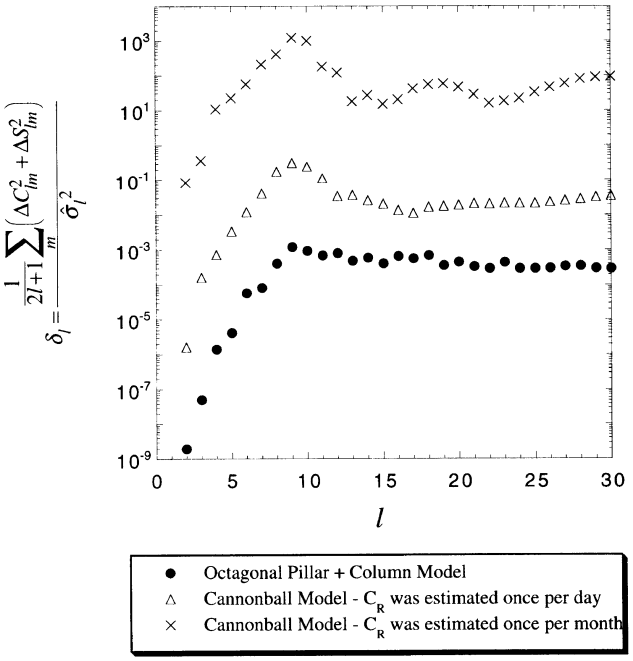


Fig. 6. Relative error of the estimated lunar gravity field coefficients from the reference gravity field model, LUN60d (Konopliv *et al.*, 1993).

model. Even for the low degree coefficients, there is a two orders of magnitude improvement in $\delta_l$. These results show the improvement of our new radiation pressure model over the cannonball model. However, it should be noted that the result was obtained from the tracking data of only one spacecraft. If we would include tracking data of other spacecraft such as Clementine, the Apollo 15 and 16 subsatellites, Lunar Orbiter I–V, and Lunar Prospector, along with SELENE, this difference may become smaller.

## 5. Summary

A new solar radiation pressure model of the relay satellite has been constructed. In the new model, the shape of the satellite is assumed to be a combination of an octagonal pillar and a column. The optical properties of the surface materials which cover each part of the spacecraft are taken into account. The forces due to the solar radiation pressure on these two parts are computed independently and the total acceleration on the satellite center of mass is obtained as the vectorial sum of these two components. Simulation of the tracking data reduction has shown that we can reduce the observation residuals using the new radiation pressure model compared to standard cannonball modeling techniques. Moreover, simulated estimation of selenopotential coefficients shows that our new model can also decrease the errors in coefficients significantly compared to the results obtained by the cannonball model. The difference between two models is come from the anisotropic component of acceleration which is normal to the sun-satellite direction. It is therefore concluded that our new radiation pressure model will be very useful not only for the improvement of the orbit determination accuracy of the relay satellite but also for the precise lunar gravitational coefficients estimation.

Finally, some factors needed to improve the radiation pressure model are described. The variation in direction of spin axis seems to be the largest error source in the model. At the time of orbit insertion, the spin axis is planned to aligned to be perpendicular to the lunar orbital plane. The torque on the spacecraft due to the lunar gravitation and solar radiation pressure slowly alters the direction of the spin axis, but its manner has not been well understood till date. As can be seen in Fig. 3, the acceleration due to the radiation pressure depends strongly on the angle between the spin axis and the direction to the Sun. Therefore, future work should investigate the how spin axis direction changes with time, and subsequently, incorporate this in the model. The specular and diffuse reflectivities of the surface material may be another major error source in the model. The values used here are the same as those used to develop the "macromodel" of TOPEX/Poseidon (Antreasian and Rosborough, 1992). The reflectivities of the relay satellite may be different even if the surface is covered by the same materials as TOPEX/Poseidon. The refrectivities of surface materials of the "real" relay satellite should be measured before launch. Moreover, if the plate is covered with two or more different materials, we have to compute mean reflectivities using a weighted sum by the area that each material occupies. In other words, if surface materials are chosen to diminish the acceleration normal to the sun-satellite line, detailed radiation pressure model may be unnecessary to achieve the required orbit accuracy. Furthermore, the effect of self shadowing may also become an error source. The area of the shadow on some part of the surface by the other part of the spacecraft is a very complicated function of $\theta$, the angle between the spin axis and the direction to the Sun. Therefore, some simplification might be necessary in including such effects. Finally, it is very important to simulate the four-way Doppler data reduction process and examine how the error in the solar radiation pressure model of the relay satellite affects the precision of the lunar gravity field recovery.

**Acknowledgments.** The authors wish to express his gratitude to Drs. Kousuke Heki and Koji Matsumoto of the National Astronomical Observatory for their useful advice on the tracking data reduction of SELENE. They are also grateful to David Rowlands of NASA/GSFC for the kind instructions of utilizing GEODYN-II. They acknowledge the careful readings and helpful comments by the reviewers.

## References

Antreasian, P. G. and G. W. Rosborough, Prediction of radiant energy forces on the TOPEX/POSEIDON spacecraft, *J. Spacecr Rockets*, **29**, 81–92, 1992.

Kaula, W. M., *Theory of Satellite Geodesy*, 120 pp., Blaisdell, Waltham, MA, 1966.

Konopliv, A. S., W. L. Sjogren, R. N. Wimberly, R. A. Cook, and A. Vijayaraghavan, A high resolution lunar gravity field and predicted orbit behavior, in *AAS/AIAA Astrodynamics Specialist Conference*, **Pap. # AAS 93-622**, Victoria, B.C., August, 1993.

Kubo-oka, T., Long-term effect of solar radiation on the orbit of an octagonal satellite orbiting around the moon, *Adv. Space Res.*, **23**(4), 727–731, 1999.

Lemoine, F. G. R., D. E. Smith, M. T. Zuber, G. A. Neumann, and D. D. Rowlands, A 70th degree lunar gravity model (GLGM-2) from Clementine and other tracking data, *J. Geophys. Res.*, **102**(E7), 16339–16359, 1997.

Matsumoto, K., K. Heki, and D. D. Rowlands, Impact of far-side satellite tracking on gravity estimation in the SELENE project, *Adv. Space Res.*, 1999 (in press).

McCarthy, D. D. (ed.), *IERS Standards*, 150 pp., IERS Technical Note, 13,

1992.
Milani, A., A. M. Nobili, and P. Farinella, *Non-gravitational Perturbations and Satellite Geodesy*, 125 pp., Universita di Pisa, Italy, 1987.
Pavlis, D. E., S. Luo, P. Dahiroc, J. J. McCarthy, and S. B. Luthke, *GEODYN-II, Operations Manual*, 428 pp., Greenbelt, Maryland, 1998.
Sengoku, A., On lunar gravitaitonal potential recovery from SELENE satellites, *Proc. 30th Symposium on Celestial Mechanics*, **30**, 131–136, 1998.
Sengoku, A., M. K. Cheng, and B. E. Schutz, Anisotropic reflection effect on satellite, Ajisai, *J. Geodesy*, **70**, 140–145, 1995.
Standish, E. M., X. X. Newhall, J. G. Williams, and W. F. Folkner, JPL Planetary and Lunar Ephemerides, DE403/LE403, *JPL IOM*, **314**, 10–127, 1995.
Ullman, R. E., SOLVE Program, *NASA Contract Report NAS5-29393, Task 503*, 36 pp., Greenbelt, Maryland, 1992.

T. Kubo-oka (e-mail: tkubooka@aa.mbn.or.jp) and A. Sengoku (e-mail: asengoku@cue.jhd.go.jp)